Acta Crystallographica Section B
Structural Science
ISSN 0108-7681

Pressure-frozen benzene I revisited

Armand Budzianowski and Andrzej Katrusiak*

Faculty of Crystal Chemistry, Adam Mickiewicz University, Grunwaldzka 6, 60-780 Poznań, Poland

Correspondence e-mail: katran@amu.edu.pl

Received 3 October 2005
Accepted 14 November 2005

The crystal structure of benzene, C_6H_6, *in situ* pressure-frozen in phase I, has been determined by X-ray diffraction at 0.30, 0.70 and 1.10 GPa, and 296 K. The molecular aggregation within phase I is consistent with van der Waals contacts and electrostatic attraction of the positive net atomic charges at the H atoms with the negative net charges of the C atoms. The C—H···aromatic ring centre contacts are the most prominent feature of the two experimentaly determined benzene crystal structures in phases I and III, whereas no stacking of the molecules has been observed. This specific crystal packing is a likely reason for the exceptionally high polymerization pressure of benzene. The changes of molecular arrangement within phase I on elevating the pressure and lowering the temperature are analogous.

1. Introduction

Benzene is one of the most renowned chemical substances. Its molecular structure led to the concept of aromaticity. Equally intriguing are the intermolecular interactions and associations of benzene. Apart from van der Waals forces, two other main types of interactions are considered:

(i) the electrostatic attraction between H atoms bearing a positive partial net atomic charge with the π electrons of the neighbouring molecules (Williams *et al.*, 1992);

(ii) the hydrogen bonds between the H atoms and aromatic π electrons (Levitt & Perutz, 1988; Steiner *et al.*, 1995; Burley & Petsko, 1986; Green, 1974).

These possible interactions have to compromise with the close-packing condition of molecules in the crystal (Cox *et al.*, 1958; Kitajgorodski, 1976). The first reports on the physico-chemical properties of benzene at atmospheric pressure, such as melting point, thermal expansion and latent heat (*e.g.* Demerliac, 1898; Ferche, 1891), as well as the studies at elevated pressure (Tammann, 1903), date back to the turn of the nineteenth and twentieth centuries. At the beginning of the twentieth century Bridgman (1914*a*,*b*) carried out several experiments on benzene at pressures up to 1.25 GPa between 273 and 473 K, and a pressure-induced transition between solid-state phases was discovered. Later the study of compression and the relative volume of benzene as a function of temperature and pressure was extended to 5 GPa (Bridgman, 1931, 1942, 1949). The crystal structure of benzene was first determined at 270.15 K at ambient pressure by Cox *et al.* (1958). Six years later the structure of benzene at 138.15 and 218.15 K was studied by neutron diffraction (Bacon *et al.*, 1964), and in 1987 deuterated benzene (C_6D_6) was studied at 123 and 15 K (Jeffrey *et al.*, 1987). More recently new solid-state phases of benzene were suggested from calorimetry, optical observations, IR, far-IR, Raman spectroscopy and X-

ray powder diffraction (van Eijck *et al.*, 1998; Thiéry & Léger, 1988; Cansell *et al.*, 1993, and references therein). Owing to its simple, highly symmetric and rigid molecular structure, benzene has become the model structure for calculating the lattice-mode vibrations in molecular crystals (Harada & Shimanouchi, 1967; Bonadeo & Taddei, 1973; Taddei *et al.*, 1973; Ellenson & Nicol, 1974; Burgos *et al.*, 1975).

Benzene was also one of the first pressure-crystallized liquids investigated by single-crystal X-ray diffraction in a diamond–anvil cell (DAC; Weir *et al.*, 1969; Piermarini *et al.*, 1969). The crystal of the benzene phase described by Bridgman as phase I, stable from 68 MPa to $\sim$ 1.3 GPa, was studied at 0.07 GPa and 293 K, and identified as equivalent to the low-temperature phase (270–15 K): space group *Pbca*, Z = 4 (Weir *et al.*, 1969; Piermarini *et al.*, 1969). However, until now no structural information on phase I at high pressure has been available in the literature or any of the databases. There is also some confusion with regard to phases II and III of benzene.

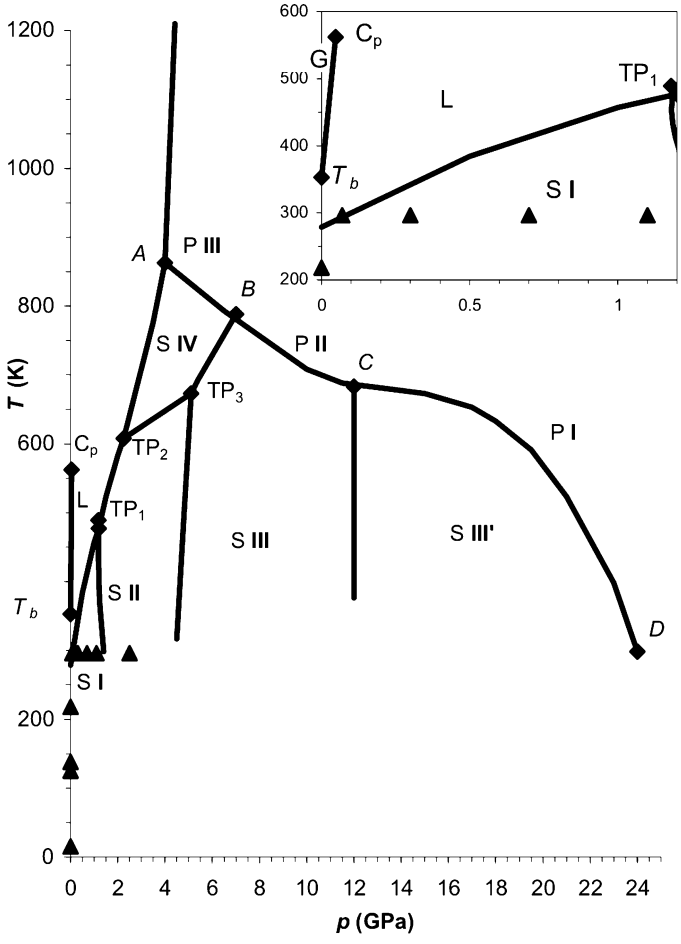

Figure 1
Phase diagram of benzene compiled from the experimentally observed transformations. L denotes a liquid; G a gas; S I–IV the solid-state phases, P I–III the polymers. The triple points are denoted as TP_1 [1.20 (5) GPa and 477 K; Akella & Kennedy, 1971], TP_2 [2.25 (5) GPa and 608 (5) K; Akella & Kennedy, 1971], TP_3 (5.1 GPa and 697 K; Cansell *et al.*, 1993). T_b is the boiling point at 299 K and 0.1 MPa; C_p is the critical point at 4.89 MPa and 562 K (Tsonopoulos & Ambrose, 1995). Points *A*, *B*, *C* and *D* outline the polymerization region – see the text. The inset magnifies the 200–600 K and 0–1.2 GPa region.

Piermarini *et al.* (1969) reported a benzene structure at 2.5 GPa and 293 K which they labelled *phase II*: it is monoclinic, space group $P2_1/c$, Z = 2. However, more recent powder diffraction, calorimetric and Raman spectroscopy studies (Thiéry & Léger, 1988; Akella & Kennedy, 1971) showed that this structure should be labelled as phase III, existing between $\sim$ 4.0 (5) and 11 (1) GPa, because another phase observed at lower pressure between 1.4 (1) and 4.0 (5) GPa was labelled as phase II. Its powder diffraction pattern could not be indexed in the $P2_1/c$ monoclinic structure described by Piermarini *et al.* (1969), whereas the powder diffraction pattern of benzene above 4.0 GPa fitted perfectly to those data. In accordance with these recent studies, in this report the crystal structure of benzene determined by Piermarini *et al.* (1969) at 2.5 GPa will be denoted as phase III. Presently it appears that the likely reasons for the discrepancies between the structural and spectroscopic reports may be due to the persistence of the metastable phase III below 4 GPa (Boldyreva *et al.*, 2000, 2002; Katrusiak, 1995) or some trivial calibration or interpretation inaccuracies.

The existence of another phase of benzene between 11 (1) and 24 GPa, described as a distorted structure of phase III and denoted III′ (Thiéry & Léger, 1988), is hard to reconcile with the observations that unsaturated bonds become extremely reactive above 10 GPa (Nicol & Yin, 1984). Such a behaviour would indicate that the aromatic systems are much more stable than localized double bonds or that the crystal environments in the benzene phases stabilize the molecular structure. There are even reports that pressures as high as nearly 24 GPa are required to induce polymerization, resulting in a three-dimensional saturated polymer (Akella & Kennedy, 1971). In the phase diagram of benzene in Fig. 1, points *A* (at 4.0 GPa and 863 K; Block *et al.*, 1970), *B* (at 7.0 GPa and 788 K; Cansell *et al.*, 1993), *C* (at 12.0 GPa and 683 K; Cansell *et al.*, 1993) and *D* (24.0 GPa and 298 K; Cansell *et al.*, 1993) outline the polymerization region. This phase diagram of benzene is completed by phase IV (Cansell *et al.*, 1993) of a still unknown structure, which transforms from phase II above 510 K, and from phase III above 673 K.

There are certain discrepancies between the phase diagram compiled in Fig. 1 and that reported by Piermarini *et al.* (1969). For example, they reported the pressure and temperature of the triple point between phases I, II and liquid at 3.0 GPa and 583 K. The reason for this difference may be due to the different techniques used for performing those measurements. The results obtained by using an isobaric cylinder and piston set-up (Bridgman, 1911), a piston-cylinder apparatus (Akella & Kennedy, 1971) and a membrane DAC (Cansell *et al.*, 1993) are consistent. Meanwhile Piermarini *et al.* (1969) used a DAC operated by tightening screws, which to a good approximation produces isochoric conditions (the thermal expansion of the high-pressure chamber is negligibly small compared with the thermal expansion of molecular solids). For such a heated screw-driven DAC the pressure strongly depends on temperature. When this p–T interdependence was taken into account, our observations in the screw-driven DAC become consistent with the results of piston-and-cylinder experiments.

The pioneering high-pressure structural studies of benzene phases I and III were performed with a precession camera using a photographic technique (Weir *et al.*, 1969; Piermarini *et al.*, 1969). It was postulated by comparing the unit-cell dimensions of the pressure-frozen crystal, and without solving its structure, that it is consistent with the low-temperature structure of phase I (Cox *et al.*, 1958). The structure model of phase III was solved by comparing the *R* factors of 19 observed reflections for the rigid benzene molecule at various orientations about the inversion centre (Piermarini *et al.*, 1969). After 2 years the rigid-molecule structure of phase III was optimized by the Monte Carlo fit to the same previously measured data (Fourme *et al.*, 1971). There is still no experimental information about the crystal structures of phase II, stable between 1.4 (1) and 4.0 (5) GPa, nor for phase IV (*cf.* Fig. 1). When this paper was being prepared for submission, the extensive theoretical study of benzene crystal structures was reported (Raiteri *et al.*, 2005). Within the framework of the experimentally determined phase diagram one additional phase has also been postulated and arrangements for those phases for which structures have been not determined by experimental methods have been calculated.

The main aim of this study was to determine the structure of pressure-frozen benzene in phase I, and to follow its changes as a function of pressure. The molecular association, considerably modified in the compressed molecular crystal, can reveal the interplay between directional (hydrogen bonding) and non-directional (electrostatic and van der Waals) intermolecular interactions of this classical molecule, and their role in the molecular association and structural transformations of the crystals. Phase I is ideal for the purpose of revealing the role of intermolecular interactions in the association of benzene molecules, whereas at the higher-pressure phases the factor of close packing is bound to become more dominant. Besides, only for phase I can the temperature- and pressure-frozen structures be compared.

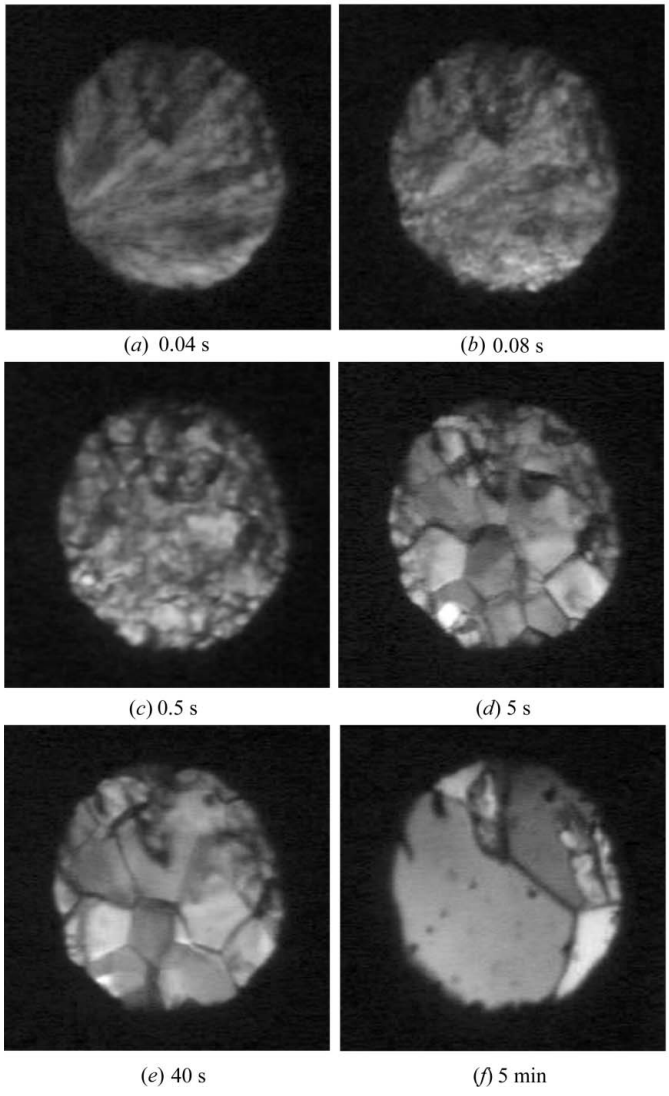

Figure 2
Benzene pressure-frozen in phase I at (*a*) 296 K and 0.07 GPa, and (*b*)–(*f*) the time evolution of the spontaneous re-crystallization process inside the DAC at 296 K and 0.07 GPa. The time-lapses from the moment of freezing are given below the photographs.

2. Experimental

The *in situ* pressure-freezing process began at above ~ 0.07 GPa, when benzene froze in the form of the polycrystal resembling a crashed glass (Fig. 2*a*). Immediately after the small crystal grains with sharp edges started to grow at the cost of their neighbours (their edges became less sharp; Fig. 2), and finally after a few minutes several crystals stabilized in the chamber. This behaviour testifies to the strong dynamics of the benzene molecules at 296 K, but may also be an indication of the existence of a metastable phase. To obtain the single crystal, the DAC (Merrill & Bassett, 1974) had to be heated to obtain one crystal grain, and then cooled slowly. The observed morphologies of the crystal in the process of heating and cooling the DAC, globular at high temperature and with developed faces at lower temperatures (Fig. 3), are similar to

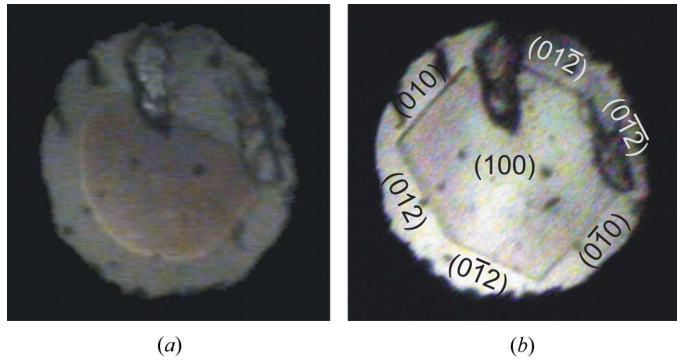

Figure 3
Two characteristic morphologies of the benzene crystals in phase I: (*a*) the globular single crystal at ~ 0.3 GPa and 310 K; (*b*) a single crystal with well developed faces at about 400 K, growing at isochoric conditions in the DAC after benzene was pressure-frozen at *ca* 100 MPa at room temperature and then heated to melting, except for one grain. Two ruby chips for pressure calibration are visible at the top and right edges of the DAC chamber.

Table 1
Crystal data and structure refinement for benzene C_6H_6 in phase I.

Pressure (GPa)		0.30 (5)	0.70 (5)	1.10 (5)
Temperature (K)		296 (2)	296 (2)	296 (2)
Formula weight		78.11	78.11	78.11
Wavelength (Å)		0.71073	0.71073	0.71073
Crystal system		Orthorhombic	Orthorhombic	Orthorhombic
Space group		*Pbca*	*Pbca*	*Pbca*
Unit-cell dimensions (Å)	*a*	7.243 (3)	7.287 (6)	7.221 (4)
	b	9.31 (2)	9.20 (2)	9.05 (2)
	c	6.756 (3)	6.688 (9)	6.590 (5)
Volume (Å ^{3})		455.6 (1)	448.4 (1)	430.7 (1)
Z		4	4	4
Calculated density (g cm^{-3})		1.136	1.154	1.202
Absorption coefficient (mm^{-1})		0.064	0.065	0.067
F(000)		168	168	168
Crystal diameter and height (mm)		0.35 and 0.1	0.35 and 0.1	0.34 and 0.1
θ range for data collection (°)		4.67–23.12	4.69–29.56	4.75–29.42
Limiting indices: *h*, *k*, *l*		$-7 \Rightarrow h \Rightarrow 6$	$-9 \Rightarrow h \Rightarrow 9$	$-9 \Rightarrow h \Rightarrow 9$
		$-5 \Rightarrow k \Rightarrow 6$	$-9 \Rightarrow k \Rightarrow 8$	$-5 \Rightarrow k \Rightarrow 5$
		$-6 \Rightarrow l \Rightarrow 5$	$-7 \Rightarrow l \Rightarrow 7$	$-8 \Rightarrow l \Rightarrow 8$
No. of reflections collected/unique (R_{int})		293/48 (0.145)	1167/179 (0.132)	1400/126 (0.151)
Completeness (to θ_{max}) (%)		15.1 (to 23.12°)	28.4 (to 29.56°)	21.2 (to 29.42°)
Refinement method		Full-matrix least-squares on F^2	Full-matrix least-squares on F^2	Full-matrix least-squares on F^2
No. of data/restraints/parameters		48/0/13	179/0/37	126/0/13
Goodness-of-fit on F^2		1.290	1.039	1.013
Final R_1/wR_2 ($I > 2\sigma_I$)		0.1316/0.2949	0.0530/0.1092	0.1418/0.2350
R_1/wR_2 (all data)		0.1316/0.2949	0.2023/0.1345	0.1754/0.2476
Largest difference peak and hole (e Å^{-3})		0.166/−0.195	0.114/−0.093	0.130/−0.122

those reported by Piermarini *et al.* (1969). In the final form at room temperature the single-crystal sample fully filled the high-pressure chamber and its dimensions were equal to those of the hole in the gasket.

The pressure inside the DAC was calibrated by the ruby-fluorescence method (Piermarini *et al.*, 1975; Mao *et al.*, 1985), using a Betsa PRL spectrometer. The single-crystal X-ray diffraction studies have been carried out with a KUMA KM4-CCD diffractometer. The crystals at 0.30 (5), 0.70 (5) and 1.10 (5) GPa were subsequently obtained by heating the DAC and reducing the chamber volume during the cooling process. The *CrysAlis* software, Version 1.171.24 (Oxford Diffraction Limited, 2002), was used for the data collections (Budzianowski & Katrusiak, 2004) and the preliminary reduction of the data. After the intensities were corrected for the effects of DAC absorption and sample shadowing by the gasket (Katrusiak, 2003, 2004), the diamond reflections were eliminated. The systematic absences unequivocally showed that the crystals are orthorhombic in the space group *Pbca* (Fig. 3*b*). The unit-cell dimensions have been corrected for the effect of gasket shadowing (Katrusiak, 2006). The structure was solved in a straightforward manner by direct methods (Sheldrick, 1990), and refined (Sheldrick, 1997) without any constraints and with isotropic temperature factors for all C atoms, except the structure at 0.7 GPa, where the anisotropic temperature factors were applied. The H atoms were calculated from the molecular geometry ($d_{C-H} = 0.97$ Å) and their U_{iso} values were constrained to $1.2U_{eq}$ of the carrier atoms. The crystal data are summarized in Table 1 and the changes of the unit-cell parameters are shown in Fig. 4. Detailed structural information have been deposited in the IUCr electronic archive.[1]

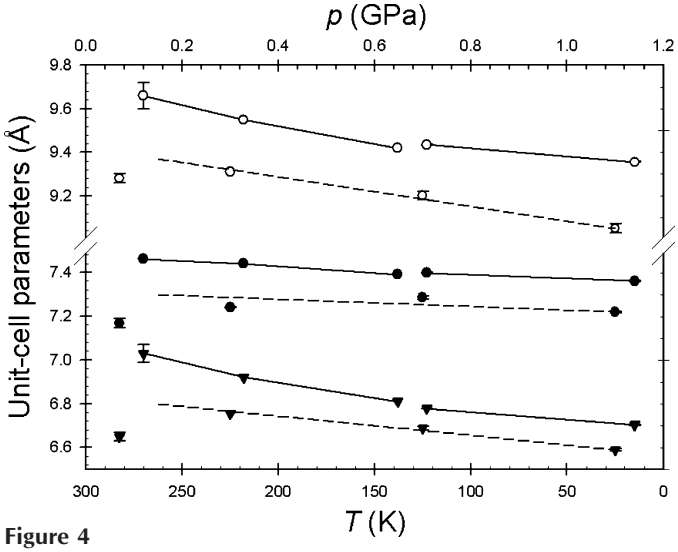

Figure 4
Unit-cell dimensions of benzene I plotted as a function of pressure (shown as dashed lines; the scale in GPa units is at the top of the plot) and as a function of temperature (the reverse scale at the bottom and solid-line plots). Low-temperature data were measured for C_6H_6 (Cox *et al.*, 1958; Bacon *et al.*, 1964) and C_6D_6 at 123 and 15 K (Jeffrey *et al.*, 1987). The unit-cell parameters measured at 0.07 GPa (Weir *et al.*, 1969) have been excluded from the regression lines, as they considerably divert from the other results – see the text.

It was apparent that the crystals at 0.30, 0.70 and 1.10 GPa were oriented differently relative to the DAC. It was previously reported that pressure-frozen liquids (*e.g.* benzene, bromine, tetrachlorocarbonate and carbon disulfide) assumed

[1] Supplementary data for this paper are available from the IUCr electronic archives (Reference: AV5045). Services for accessing these data are described at the back of the journal.

Table 2
Bond lengths (Å) and angles (°) for benzene in phase I.

	0.3 GPa	0.7 GPa	1.1 GPa
C1—C2	1.40 (4)	1.397 (8)	1.420 (16)
C2—C3	1.38 (8)	1.384 (10)	1.41 (3)
C3—C1^{i}	1.38 (5)	1.354 (10)	1.32 (2)
C3^{i}—C1—C2	117 (5)	120.7 (7)	121 (2)
C1—C2—C3	123 (4)	117.9 (7)	116.8 (14)
C1^{i}—C3—C2	120 (4)	121.4 (7)	122.0 (16)

Symmetry code: (i) $1-x, -y, -z$.

fixed (identical) orientations in the DAC (Weir *et al.*, 1969) for each compound. Due to the different orientations, different regions of the reciprocal space of the crystal were accessible, which could affect the range (the θ_{max} angles) of the significant intensity measurements (Table 1). Also, at lower pressures the thermal vibrations of atoms are stronger and hence the scattering of X-rays is weaker (Katrusiak, 1991). It appears that for these reasons the diffraction data of the structure at 0.3 GPa were insufficient for refining anisotropic displacement parameters. On the other hand, the quality of the crystal at 1.1 GPa was affected by strains in the single-crystal sample cooled over 170 K in the rigid high-pressure chamber. Hence, the isotropic displacement parameters had to be used for the C atoms in the 1.1 GPa model.

3. Results

The unit-cell dimensions (Fig. 4), crystal symmetry and atomic positions determined in this study confirm that the pressure-frozen structure is consistent with phase I of benzene frozen by cooling below its m.p. at ambient pressure (0.1 MPa). The plots in Fig. 4 also include the parameters measured by Weir *et al.* (1969), assigned by those authors to 0.7 kbar (*i.e.* 0.07 GPa). Their parameters apparently do not fit the presently measured pressure dependence of the unit-cell dimensions, but would be more consistent if the pressure was changed to 0.7 GPa. The molecular dimensions in I are listed in Table 2.

The crystal structure of benzene I can be considered as being built of layers which are perpendicular to [010] of the molecules having the shortest intermolecular C···H contacts, as illustrated in Fig. 5. It is characteristic that the molecules in such layers are arranged nearly perpendicular – inclined by 84 (2)° at 0.3 GPa, by 88.5 (4)° at 0.7 GPa and by 89.1 (11)° at 1.1 GPa – to their neightbours (Fig. 6). It can be seen that for a given molecule within the layer there are two such perpendicular neighbouring molecules, one of each side of its ring. Each of these perpendicular molecules interact with the ring through two H atoms, one of which is directed at the centre of the ring, the other at a C atom. The other close contacts are to the molecules in the neighbouring layers along [010] – compare Figs. 5, 6 and 7. It can be observed that when pressure increases, these distinctive features of the benzene-molecule interactions remain unchanged, except for the gradual shortening of the contacts, as illustrated by the colour decoration of the Hirshfeld surface (McKinnon *et al.*, 2004) in Figs. 8(*a*)–(*c*).

The molecules interact mainly *via* H···C and H···H contacts (the red-coloured indentations in Figs. 7 and 8). The gradual changes on the Hirshfeld surface indicate that the interactions are monotonically modified along with the crystal environment without abrupt rearrangements of the molecules within the pressure range of phase I. In both phases I and III the molecules are located at the inversion centres, thus the molecular environment is also symmetric.

The new molecular arrangement in phase III also preserves certain characteristic features of phase I. For example, the close $H^{\delta+}\cdots\pi$ electron interactions are clearly visible at the centres of the rings as the red-coloured deepest depression on the Hirshfeld surfaces, shown in Figs. 8(*a*)–(*d*).

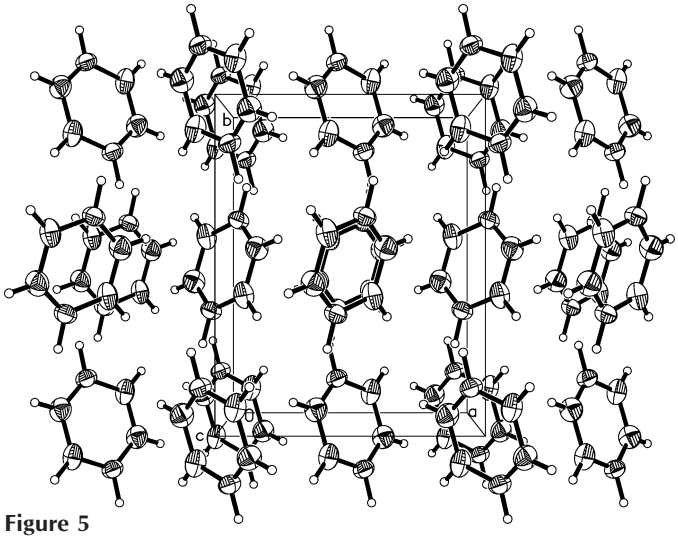

Figure 5
Autostereogram (Katrusiak, 2001*a*,*b*) of the benzene I structure at 0.7 GPa viewed down [001]. The thermal ellipsoids have been drawn at the 50% probability level, and the H atoms have been shown as spheres of arbitrary radius.

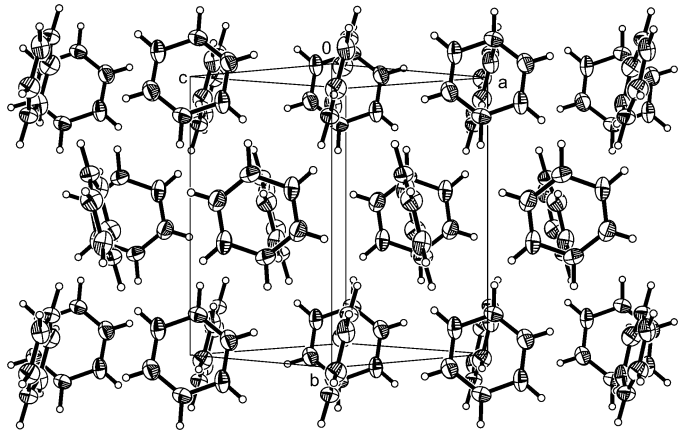

Figure 6
Autostereogram (Katrusiak, 2001*a*,*b*) of the benzene I structure at 0.7 GPa viewed down [101]. The thermal ellipsoids have been drawn at the 50% probability level, and the H atoms have been shown as spheres of arbitrary radius.

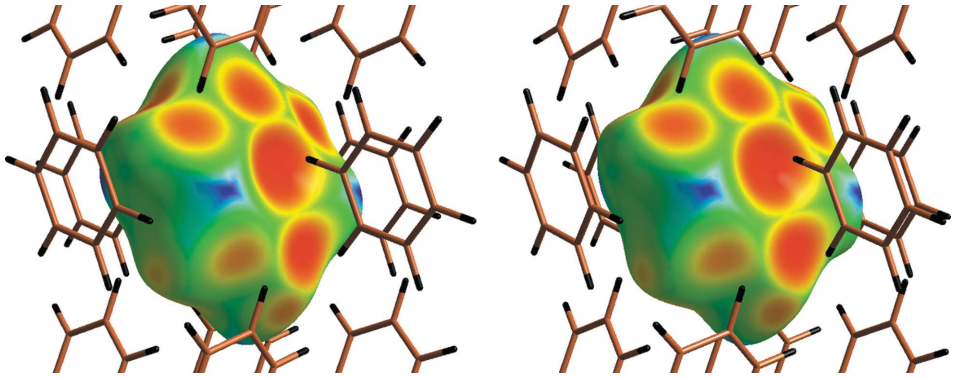

Figure 7
A stereoscopic view of one benzene molecule in phase I at 138 K and 0.1 MPa represented as a Hirshfeld surface. The colour scale on the Hirshfeld surface represents the close intermolecular distances (red for the shortest, blue for the longest). The crystal [010] axis is vertical in this drawing and the viewing direction is at *ca* 30 and 60° to the [100] and [001] axes, respectively.

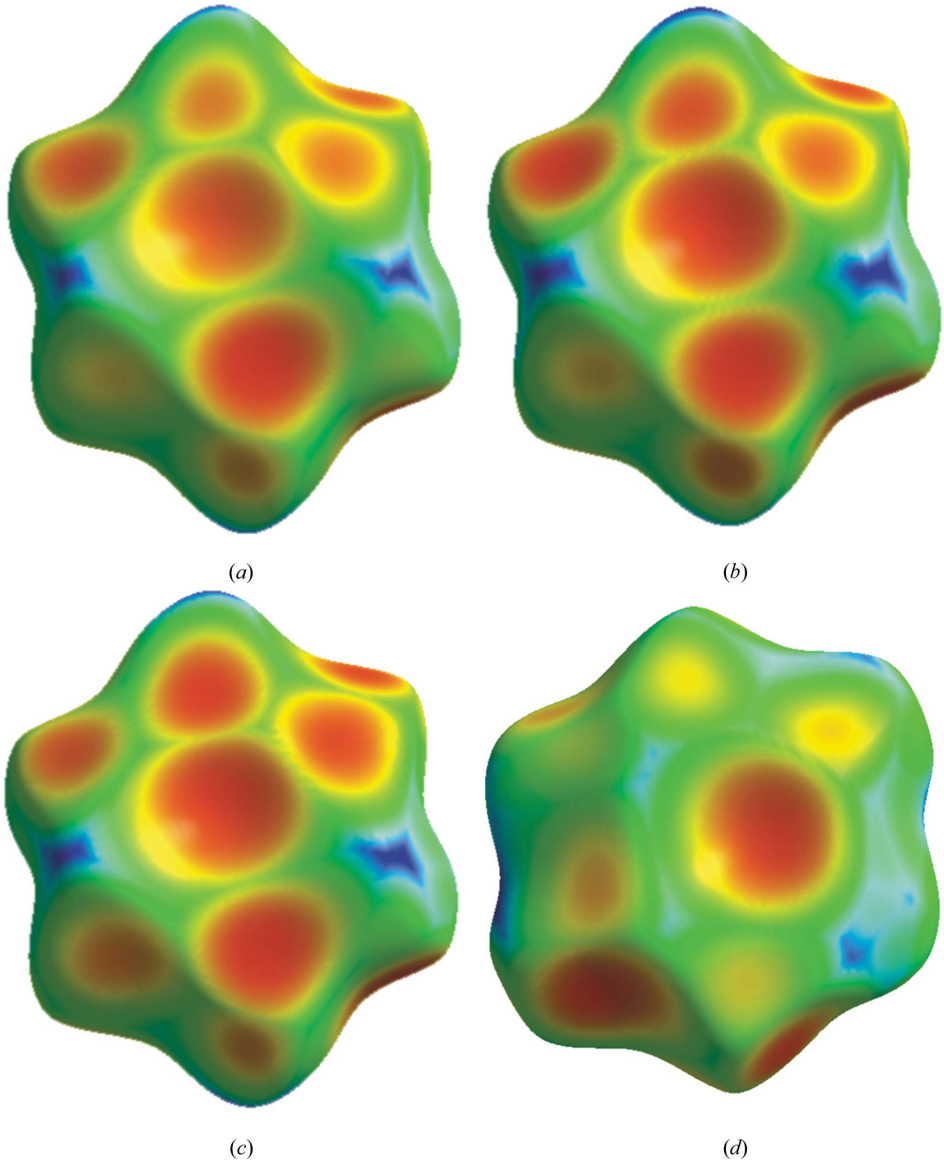

Figure 8
The interactions of the benzene molecule represented as a colour scale on the Hirshfeld surface at 296 K: (*a*) in phase I at 0.3 GPa; (*b*) 0.7 GPa; (*c*) 1.1 GPa; (*d*) in phase III at 2.5 GPa.

The intermolecular interactions can be characterized by the closest contacts in the structure – their pressure and temperature dependence is plotted in Fig. 9. In this plot the shortest intermolecular contacts at 0.3 GPa and 296 K have been arranged in ascending order, and then the contacts at other conditions of p/T have been plotted for the same sequence of contacts. It can be immediately observed that the contacts differentiate when pressure increases and this initially monotonic plot becomes undulated. This illustrates that when the crystal is compressed some contacts shorten and others lengthen, and the structure stable at 0.3 GPa becomes considerably strained. The differences between the lengthened and shortened interatomic contacts approach 0.4 Å at 1.1 GPa. These strains are relieved when the molecules are rearranged at the phase transition at 1.4 GPa.

The orientation of the benzene molecules in the crystal structure has been described by the angles between the benzene ring plane and the crystallographic planes (100), (010) and (001) (Fig. 10*a*), and by the angles between the vector joining the ring centre and the C1 atom, and axes [100], [010] and [001] (Fig. 10*b*). The latter set of three angles describes the benzene-ring orientation about its C_6 axis (of the idealized molecule). It can be seen that the molecular orientation is hardly changed between 0.3 and 1.1 GPa. The absence of any significant rotations of the molecules within phase I, when the crystal is compressed to nearly 85% of its initial volume [V_m = 126.65 Å^3 at 0.1 MPa and 270 K (Cox *et al.*, 1958)], indicates that there are no significant changes in the molecular interactions. It can be noted that the crystal structures of benzene I at the temperature close to the melting point at 0.1 MPa, and close to the melting pressure

at 296 K differ by up to $\sim 3^\circ$, whereas the molecular orientations become similar at lower temperatures and higher pressures (see Fig. 10). Such a monotonic compression of the structure built of rigid molecules which change their orientation by only a few degrees inevitably leads to a differentiation of intermolecular contacts, as discussed above (Fig. 9).

Surprisingly, no ring stacking, which is the molecular arrangement of planar aromatic moieties very often observed in crystals, is present in the experimentally determined phases I or III (Piermarini *et al.*, 1969), or in all the theoretically predicted phases of benzene (Raiteri *et al.*, 2005). The pressure dependence of the benzene structures shows that molecular stacking does not compete with other interactions in phase I. These results suggest that no attractive interactions can be realised in the form of the stacking arrangement of benzene molecules. At the same time, the molecular environment effect of the structures dominated by H···C and H···H contacts is a likely reason for the exceptionally high polymerization pressure of benzene.

4. Conclusions

It appears that the relatively stable crystal structure of benzene below 1.1 GPa in phase I is due to the specific arrangement and interactions of the molecules. The most characteristic feature of this arrangement, the H···aromatic ring centre, can be classified as a weak hydrogen bond and is also present in the benzene III structure. This hydrogen-bond-like feature of the H···centroid interactions is absent in the homologous structures of naphthalene, anthracene and phenanthracene, as pointed out by McKinnon *et al.* (2004). The persistence of the H···aromatic ring centre interaction contacts in two different phases of benzene is an indication that these contacts may contribute considerably to the molecular attraction and crystal cohesion forces. The formation of the H···centroid contacts is easier for small molecules, like benzene, whereas the structures of large molecules have to conform to the requirements of the close-packing rule. On the other hand, the H···centroid interactions in benzene structures I and III may also be consistent with the close-packing rule, whereas the stacking arrangement may be inconsistent with it. Therefore, it is essential to continue the determinations of other structures of benzene and to clarify the ambiguities in the phase diagram of this intriguing compound.

This study was supported by the Polish Ministry of Scientific Research and Information Technology, Grant No. 3T09A18127.

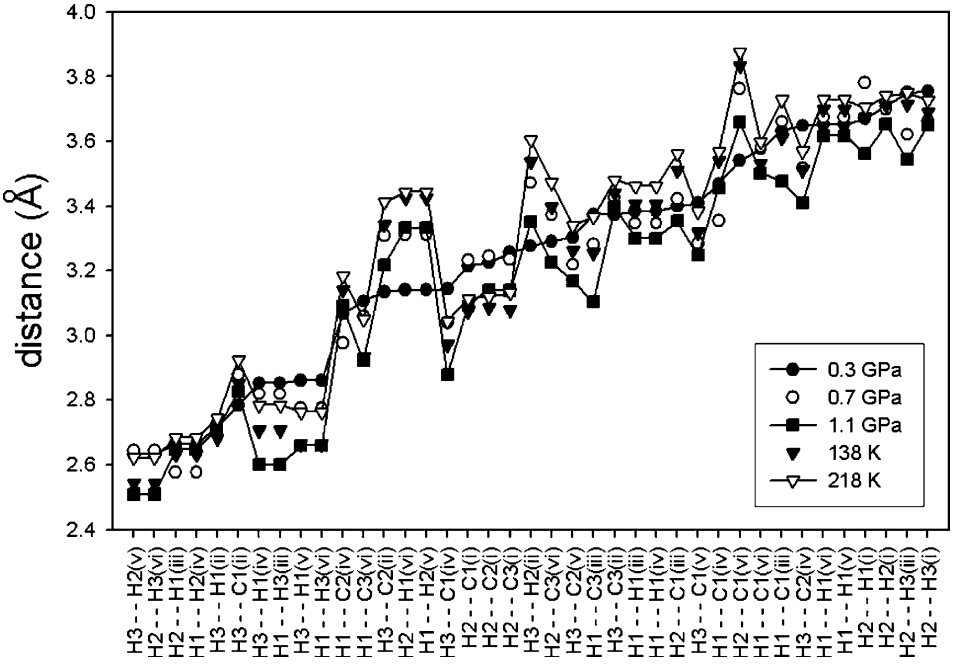

Figure 9
The differentiation of the shortest intermolecular contacts in benzene I at 296 K when pressure increases from 0.3 to 0.7 GPa and to 1.1 GPa; as well as at 218 K and 0.1 MPa, and 138 K and 0.1 MPa. Symmetry codes: (i) $-\frac{1}{2}+x, y, \frac{1}{2}-z$; (ii) $\frac{1}{2}+x, y, -\frac{1}{2}-z$; (iii) $x, \frac{1}{2}-y, \frac{1}{2}+z$; (iv) $x, \frac{1}{2}-y, -\frac{1}{2}+z$; (v) $\frac{1}{2}+x, \frac{1}{2}-y, -z$; (vi) $-\frac{1}{2}+x, \frac{1}{2}-y, -z$.

References

Akella, J. & Kennedy, G. C. (1971). *J. Chem. Phys.* **55**, 793–796.
Bacon, G. E., Curry, N. A. & Wilson, S. A. (1964). *Proc. R. Soc. A*, **279**, 98–110.
Block, S., Weir, C. E. & Piermarini, G. J. (1970). *Science*, **169**, 586–587.
Boldyreva, E. V., Shakhtshneider, T. P., Vasilchenko, M. A., Ahsbahs, H. & Uchtmann, H. (2000). *Acta Cryst.* B**56**, 299–309.
Boldyreva, E. V., Shakhtshneider, T. P., Ahsbahs, H., Sowa, H. & Uchtmann, H. (2002). *J. Therm. Anal. Calorim.* **68**, 437–452.
Bonadeo, H. & Taddei, G. (1973). *J. Chem. Phys.* **58**, 979–984.
Bridgman, P. W. (1911). *Proc. Am. Acad. Arts Sci.* **47**, 347–438.
Bridgman, P. W. (1914*a*). *Phys. Rev.* **3**, 126–141.
Bridgman, P. W. (1914*b*). *Phys. Rev.* **3**, 153–203.
Bridgman, P. W. (1931). *Proc. Am. Acad. Arts Sci.* **66**, 185–223.
Bridgman, P. W. (1942). *Proc. Am. Acad. Arts Sci.* **74**, 399–424.
Bridgman, P. W. (1949). *Proc. Am. Acad. Arts Sci.* **77**, 129–146.
Budzianowski, A. & Katrusiak, A. (2004). *High-Pressure Crystallography*, edited by A. Katrusiak & P. F. McMillan, pp. 157–168. Dordrecht: Kluwer Academic Publishers.
Burgos, E., Bonadeo, H. & D'Alessio, E. (1975). *J. Chem. Phys.* **63**, 38–47.
Burley, S. K. & Petsko, G. A. (1986). *FEBS Lett.* **203**, 139–143.
Cansell, F., Fabre, D. & Petitet, J. P. (1993). *J. Chem. Phys.* **99**, 7300–7304.
Cox, E. G., Cruickshank, D. W. J. & Smith, J. A. S. (1958). *Proc. R. Soc. London A*, **247**, 1–21.
Demerliac, R. (1898). *Jour. de Phys.* **7**, 591.
Eijck, B. P. van, Spek, A. L., Mooij, W. T. M. & Kroon, J. (1998). *Acta Cryst.* B**54**, 291–299.

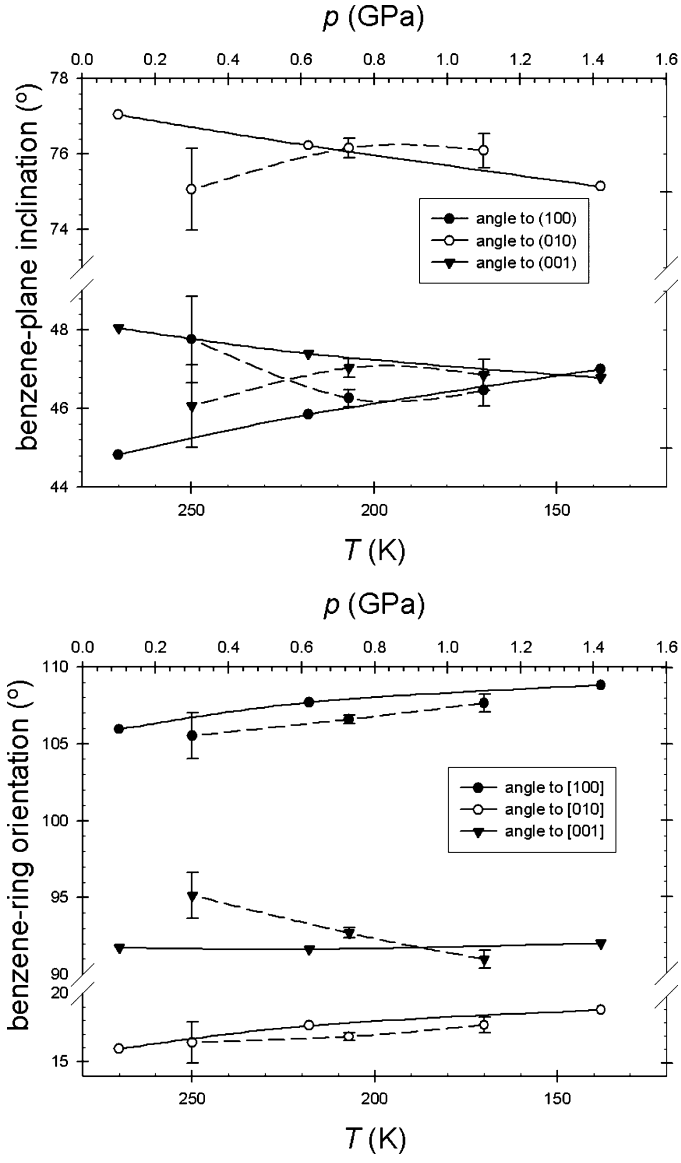

Figure 10
The pressure (dashed lines) and temperature (solid lines) dependences of the benzene molecule orientation in phase I described by the inclination angles of the ring plane to the unit-cell planes (upper), and by the angles between the cell axes and the vector from the ring centre to the C1 atom.

Ellenson, W. D. & Nicol, M. (1974). *J. Chem. Phys.* **61**, 1380–1389.
Ferche, J. (1891). *Ann. Phys.* **44**, 265.
Fourme, R., Andre, D. & Renaud, M. (1971). *Acta Cryst.* B**27**, 1275–1276.
Green, R. D. (1974). *Hydrogen Bonding by C—H Groups.* New York: Wiley Interscience.
Harada, I. & Shimanouchi, T. (1967). *J. Chem. Phys.* **46**, 2708–2714.
Jeffrey, G. A., Ruble, J. R., McMullan, R. K. & Pople, J. A. (1987). *Proc. R. Soc. A*, **414**, 47–57.
Katrusiak, A. (1991). *Cryst. Res. Technol.* **26**, 523–531.
Katrusiak, A. (1995). *Acta Cryst.* B**51**, 873–879.
Katrusiak, A. (2001*a*). *J. Mol. Graph. Model.* **19**, 363–367.
Katrusiak, A. (2001*b*). *J. Mol. Graph. Model.* **19**, 398.
Katrusiak, A. (2003). *REDSHAD*. Adam Mickiewicz University, Poznań.
Katrusiak, A. (2004). *Z. Kristallogr.* **219**, 461–467.
Katrusiak, A. (2006). In preparation.
Kitajgorodski, A. I. (1976). *Kryształy molekularne*, p.45. Warsaw: PWN (in Polish).
Levitt, M. & Perutz, M. F. (1988). *J. Mol. Biol.* **201**, 751–754.
Mao, H. K., Xu, J. & Bell, P. M. (1985). *J. Geophys. Res.* **91**, 4673–4676.
McKinnon, J. J., Spackman, M. A. & Mitchell, A. S. (2004). *Acta Cryst.* B**60**, 627–668.
Merrill, L. & Bassett, W. A. (1974). *Rev. Sci. Instrum.* **45**, 290–294.
Nicol, M. & Yin, G. Z. (1984). *J. Phys. Colloq.* **45**, 163–172.
Oxford Diffraction Limited (2002). *User Manual Xcalibur Series Single Crystal Diffractometers*, Version 1.3. Oxford Diffraction, Wrocław, Poland.
Piermarini, G. J., Block, S., Barnett, J. D. & Forman, R. A. (1975). *J. Appl. Phys.* **46**, 2774–2780.
Piermarini, G. J., Mighell, A. D., Weir, C. E. & Block, S. (1969). *Science*, **165**, 1250–1255.
Raiteri, P., Martoňák, R. & Parrinello, M. (2005). *Angew. Chem. Int. Ed.* **44**, 3769–3773.
Sheldrick, G. M. (1990). *Acta Cryst.* A**46**, 467–473.
Sheldrick, G. M. (1997). *SHELX*97. University of Göttingen, Germany.
Steiner, T., Starikov, E. B., Amado, A. M. & Teixeira-Dias, J. J. C. (1995). *J. Chem. Soc. Perkin Trans.* **2**, 1321–1326.
Taddei, G., Bonadeo, H., Marzocchi, M. P. & Califano, S. (1973). *J. Chem. Phys.* **58**, 966–978.
Tammann, G. (1903). *Kristallisieren und Schmelzen.* Leipzig: Barth.
Thiéry, M. M. & Léger, J. M. (1988). *J. Chem. Phys.* **89**, 4255–4271.
Tsonopoulos, C. & Ambrose, D. (1995). *J. Chem. Eng. Data*, **40**, 547–558.
Weir, C. E., Piermarini, G. J. & Block, S. (1969). *J. Chem. Phys.* **50**, 2089–2093.
Williams, J. H., Cockcroft, J. K. & Fitch, A. N. (1992). *Angew. Chem. Int. Ed. Engl.* **31**, 1655–1657.